ISSN 0735-2727, Radioelectronics and Communications Systems, 2019, Vol. 62, No. 9, pp. 462–473. © Allerton Press, Inc., 2019.
Russian Text © The Author(s), 2019, published in Izvestiya Vysshikh Uchebnykh Zavedenii, Radioelektronika, 2019, Vol. 62, No. 9, pp. 550–562.

Mode Mixing Suppression Algorithm for Empirical Mode Decomposition Based on Self-Filtering Method[1]

Longwen Wu[1*], Yupeng Zhang[1], Yaqin Zhao[1], Guanghui Ren[1], and Shengyang He[1]**
[1]*Harbin Institute of Technology, Harbin, China*
**ORCID: 0000-0002-6914-6695*
**ORCID: 0000-0002-0167-0597, e-mail: yaqinzhao@hit.edu.cn*

Received September 20, 2018
Revised July 30, 2019
Accepted July 30, 2019

Abstract—The Hilbert-Huang transform (HHT) is a classic method in time-frequency analysis field which was proposed in 1998. Since it is not limited by signal type, it is generally applied in medicine, target detection and so on. Empirical mode decomposition (EMD) is a pre-processing part of HHT. However, EMD still has many imperfect aspects, such as envelope fitting, the endpoint effect, mode mixing and other issues, of which the most important issue is the mode mixing. This paper proposes a mode mixing suppression algorithm based on self-filtering method using frequency conversion. The proposed algorithm focuses on the instantaneous frequency estimation and the false components removing procedures, which help the proposed algorithm to update or purify the designated intrinsic mode function (IMF). According the simulation results, the proposed algorithm can effectively suppress the mode mixing. Comparing with ensemble empirical mode decomposition (EEMD) and mask method, the suppression performance is increased by 26%.

DOI: 10.3103/S0735272719090036

1. INTRODUCTION

In order to obtain the time-frequency characteristics, the commonly used methods are short-time Fourier transform [1], fractional Fourier transform [2], wavelet transform [3] and Wigner-Ville distribution (WVD) [4–6]. Comparing with other methods, WVD has been widely used for its high time-frequency concentration. And based on the WVD, smoothing pseudo Wigner-Ville distribution (SPWVD) was proposed to eliminate cross-terms of signal time intervals in dealing with multi-component signals [7, 8].

Actually WVD can be regarded as the Fourier transform of the signal autocorrelation function, and it has high time-frequency concentration. However, when dealing with multi-component signals or non-linear frequency modulated signals, WVD always generates serious cross-terms, which may overlap with auto-terms. That is to say, WVD has a strong advantage in dealing with a single component signal, but not in dealing with the multi-component signals or non-linear frequency modulated signals [9, 10].

In order to eliminate cross-terms of signal intervals, some scholars tried to filter the signal with some designed window before using WVD. One of those methods is well known as pseudo Wigner-Ville distribution (PWVD). Since PWVD only filters signal in time domain, PWVD is not an ideal choice for suppressing cross-terms. SPWVD can eliminate cross-terms much better, because SPWVD filters signal both in time and frequency domain [11–14]. Although these smoothing versions of WVD can eliminate the effect of cross-terms in some sense, they reduce the time-frequency concentration at the same time.

It is well known that Fourier transform is suitable for linear systems and the data must be strictly periodic or stationary. However real systems are always nonlinear. When Fourier transform is directly used to analysis these data, the result makes little physical sense. Then Huang et al. proposed an analysis method named empirical mode decomposition (EMD) to decompose signal into a group of multiple one-component signals [15, 16]. After EMD, the original signal can be decomposed into multiple intrinsic mode functions (IMFs) and a residual component which characterizes the signal's time domain trend. The frequencies

[1] This work was supported by the National Natural Science Foundation of China under Grant No. 61671185.

contained in the different IMFs are in descending order from high to sub-high and from sub-high to low frequencies. In some sense, if some IMFs within certain frequency band are selected, EMD can be regarded as a filter. EMD-based methods are widely used because they are not limited by the signal's modulation form.

However, there are still some problems in the process of EMD, such as the method of envelope fitting, endpoint effect, mode mixing and other issues [17–19].

Envelope fitting is an important process in EMD. The effect of envelope fitting greatly determines the result of EMD. So it is important to choose a good method to fit envelope. There are many methods to fit envelope, such as piecewise cubic Hermite interpolation (PCHI) [20, 21], cubic spline interpolation (CSI) [15, 22], B-spline interpolation [23, 24], high-spline interpolation [25] and so on. Because the method of cubic spline interpolation can not only ensure the continuous curve of each segment, but also ensure the smoothness of the entire curve at these points, the cubic spline interpolating function has been widely used. In [26], Handa Ding compared the two methods of CSI and PCHI, and concluded that the CSI method has advantage in the signal reconstruction ability.

Endpoint effect is a common problem in the EMD. The essence of EMD method is a process of multiple siftings and finally obtaining a series of IMFs. During each sifting process, upper envelope and lower envelope are respectively obtained by fitting the signal maxima and minima using cubic spline function. Then the mean envelope is obtained according to the upper envelope and lower envelope. Since it is not possible to include both maxima and minima at the end of the signal, the upper envelope and lower envelope are inevitably divergent on both ends. With the progress of sifting process, the divergent phenomenon will pollute the data inward, and then significantly distort the final result.

In [15], Huang et al. pointed out that in order to ensure the envelope reaches the endpoint, two feature waves should be added according to the amplitude and frequency of the endpoint signal. And in [27], Huang et al. proposed a method of image closure extension of envelope. This method extends the original data sequence into a ring data symmetrically before EMD.

Another important problem is mode mixing. The problem of mode mixing always appears when there is a low-frequency sinusoidal signal with small-amplitude but high-frequency components [28]. There are several methods to suppress the mode mixing and obtain better decomposition results, such as intermittence test method [28], masking signal technique [29], the Teager energy operator [30], and the ensemble EMD (EEMD) [31]. But actually mode mixing doesn't only occur in the intermittent signal. It can also appear when signal contains time-varying frequency components. It is impossible to separate components whose frequencies locate in one octave [32].

This paper mainly focuses on the mode mixing problem in multi-component signal analysis, in which case the frequencies of the different components partly overlap. A mode mixing suppression algorithm, based on self-filtering method using frequency conversion, is exploited to obtain the every IMF whose mode mixing is suppressed efficiently. A brief description of empirical mode decomposition and several methods of parameters calculation are presented in section 2. The proposed method of self-filtering using frequency conversion is given in Section 3. Section 4 shows the simulation results of different methods. Section 5 is the concluding section.

2. EMPIRICAL MODE DECOMPOSITION AND PARAMETERS CALCULATION

2.1. Basic Principle of EMD

Empirical mode decomposition (EMD) is an empirical time-frequency analysis algorithm. The basic idea of EMD is that every signal can be transformed into a cumulative sum of multiple intrinsic mode functions (IMFs) and a residual trend according to local feature time scale of the signal. Based on this idea, Huang gives the basic conditions of IMF [15].

1. For continuous signals, the envelope formed by the minima and the envelope formed by the maxima are symmetric about the time axis.

2. For a finite continuous signal, the number of extrema and the number of zero crossings must either equal or differ at most by one.

In [15], Huang et al. proposed that even in the case of low signal-to-noise ratio (SNR), upper and lower envelopes of signal are determined by the maxima and the minima, and then the average envelope can be obtained. After EMD, the obtained IMFs represent signal components from high to sub-high and, finally, to low frequencies.

According to the conditions of IMF, it is possible to find that each IMF contains a specific vibrational mode. Moreover, the IMFs are not limited by the narrow band. So long as the signal satisfies the conditions, it is an IMF. In practical system, most signals don't satisfy the conditions of IMF, and usually contain multiple vibration forms. Therefore, for multi-component nonlinear and non-stationary time series, it is especially convenient to transform the original signal into multiple IMFs and one residual trend using EMD.

There is still a need to introduce several assumptions before decomposing the first signal:

– any signal, whether linear or non-linear, stationary or non-stationary, can be decomposed into multiple IMFs and one residual trend;

– time scale is based on time interval between adjacent extrema, that is, for FM signal, time scales at different time are not same in size, the larger instantaneous frequency is, the smaller feature time scale and vice versa;

– if the data are totally devoid of extrema but contain defects, then it can be differentiated, decomposed and reintegrated to obtain IMFs [4].

Based on the assumptions above, the decomposition process of EMD can be implemented as follows [33]:

Step 1. Identify all the local maxima and minima of signal, and fit the maxima by cubic spline interpolation as upper envelop. Repeat the procedure for the local minima to produce lower envelope. The mean of the upper and lower envelopes is designated m_1, and the difference between original signal and m_1 is h_1:

$$x(t) - m_1 = h_1. \tag{1}$$

Step 2. Check whether h_1 satisfies the conditions of IMF. If not, repeat the process in step 1, h_1 is treated as original signal. The mean of the upper and lower envelopes of h_1 is m_{11}. Then

$$h_1 - m_{11} = h_{11}. \tag{2}$$

This procedure can be repeated up to k times until the h_{1k} satisfies the conditions of IMF, h_{1k} is given by

$$h_{1(k-1)} - m_{1k} = h_{1k}, \tag{3}$$

then

$$c_1 = h_{1k} \tag{4}$$

is designated as the first IMF component.

Step 3. Separate c_1 from the rest of the signal by using

$$x(t) - c_1 = r_1. \tag{5}$$

Then treat r_1 as the original input signal, and repeat the process from step 1 to step 2. The result is

$$\begin{cases} r_1 - c_2 = r_2, \\ \vdots \\ r_{n-1} - c_n = r_n. \end{cases} \tag{6}$$

When the number of extrema of the residue, r_n, is less than three, then the entire decomposition process is completed.

Finally, original signal $x(t)$ can be expressed as

$$x(t) = \sum_{i=1}^{n} c_i(t) + r_n(t). \tag{7}$$

The component $c_i(t)$ contains the signal components from high to sub-high to low frequency. In [34], Stevenson et al. use single-component LFM signals and a three component bat echolocation pulse to analyze the quadrature characteristics of IMF, IMF consistency and residual energy at different sampling frequencies, concluding that the IMFs have more complete orthogonality at large resolution.

Based on the above analysis, it can be seen that EMD method is actually a continuous screening process, which filters one signal to be represented as multiple IMFs and one residual trend. Each IMF has only one frequency at every time, and the frequencies of different IMF components do not overlap with each other. Therefore, it is easier to deal with IMF components.

2.2. Main Problem of EMD

The analysis above shows that EMD method can get better results when dealing with non-stationary and nonlinear signals, but there are still many imperfect aspects, such as envelope fitting, the endpoint effect, mode mixing and other problems. This paper focuses on the problem of mode mixing.

In [31], Zhaohua Wu and Huang define that mode mixing occurs when one IMF contains different time-scale components or different IMF components contains signal components of one similar time-scale. As described in the introduction there are two main phenomena of mode mixing [28]. One usually exists in intermittent signal with small-amplitude but high-frequency riding wave, another happens in multi-component signals with time-varying frequency.

In order to provide better theoretical background for the second phenomenon, one signal is assumed to be

$$x(t) = A\cos(2\pi f_1 t) + A\cos(2\pi f_2 t), \tag{8}$$

where $2f_1$ equals to $(f_1 + f_2) + (f_1 - f_2)$ and $2f_2$ equals to $(f_1 + f_2) - (f_1 - f_2)$, then

$$x(t) = 2A\cos(\pi(f_1 - f_2)t)\cos(\pi(f_1 + f_2)t), \tag{9}$$

when f_1 is very close to f_2, then $f_1 + f_2 >> f_1 - f_2$, the term of $2A\cos(\pi(f_1 - f_2)t)$ becomes amplitude modulation term. In this situation, EMD method cannot effectively decompose signal, and then one IMF component will contain two or more time-scale components.

In [35], Gabriel Rilling and Patrick Flandrin drew conclusion from the study of unmodulated tones that EMD method fails to separate two tones when the ratio of lower frequency to higher frequency is greater than 0.67. In addition, they also noted that the ratio of amplitudes of the two components also affects the separation. Only when the frequency and amplitude meet the ratio criteria, can the EMD method separate components in a signal. In [29], Deering also indicates that the ratio of higher frequency to lower frequency should be greater than 2 when using EMD method.

Suppose f_1 and f_2 both are time-varying. Fig. 1 illustrates that f_1 increases with time and f_2 decreases with time. According to EMD method, the signal will be decomposed into wrong mono-component signals *CEB* and *AED* instead of the original signals *CED* and *AEB*. As f_1 and f_2 are very close near point *E*, a serious mode mixing will occur.

In order to solve the problem of mode mixing, many methods have been proposed. R. Deering proposes adding masking signal to suppress mode mixing (MS-EMD) [29]. Huang uses noise to decompose riding wave and names this method as ensemble empirical mode decomposition (EEMD) [31].

2.3. Parameters Calculation

The parameters that require calculation are the instantaneous frequency and the instantaneous amplitude. There are several methods to calculate these parameters, such as Hilbert transform, Teager transform and zero-crossing and extremum estimation.

Hilbert transform is a commonly used analytical method in time-frequency analysis. For real signal, $x(t)$, it is possible to get the corresponding analytic signal by using Hilbert transform, then obtain instantaneous amplitude, instantaneous phase and instantaneous frequency of the signal:

$$a(t) = \sqrt{x^2(t) + \hat{x}^2(t)}, \tag{10}$$

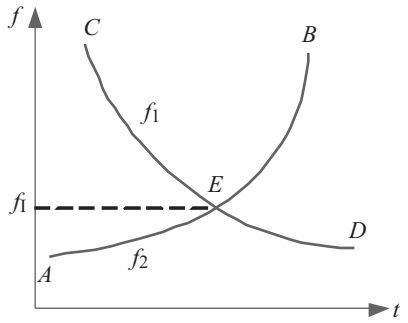

Fig. 1. Multi-component signal in time-frequency plane.

$$\phi(t) = \arctan\left(\frac{\hat{x}(t)}{x(t)}\right), \tag{11}$$

$$f(t) = \frac{\omega}{2\pi} = \frac{1}{2\pi}\frac{\mathrm{d}\phi(t)}{\mathrm{d}t}, \tag{12}$$

where $\hat{x}(t)$ is the Hilbert transform of $x(t)$.

Therefore, Hilbert transform has been widely used in the field of signal processing. However, only when the signal is a mono-component, the obtained values of instantaneous parameters using Hilbert transform could provide a meaningful representation [36].

Teager Energy Operator (TEO) is a signal analysis algorithm proposed by H. M. Teager [37]. The original purpose is to calculate and track the required energy to generate narrow-band signals when analyzing nonlinear speech signals. Nowadays it has applications in a lot of domains [38–41]. It is a nonlinear energy tracking operator, referred as Ψ. And for continuous-time signal $x(t)$ the TEO Ψ is defined as:

$$\Psi[x(t)] = [\dot{x}(t)]^2 - x(t)\ddot{x}(t)\frac{\partial^2\Omega}{\partial u^2}, \tag{13}$$

where $\dot{x}(t)$ and $\ddot{x}(t)$ are the first and the second time derivatives of $x(t)$ respectively.

According to the energy operator, instantaneous frequency and instantaneous amplitude for mono-component AM-FM (amplitude modulation–frequency modulation) signal can be written as:

$$|f(t)| \approx \frac{1}{2\pi}\sqrt{\frac{\Psi[\dot{x}(t)]}{\Psi[x(t)]}}, \tag{14}$$

$$|a(t)| = \frac{\Psi[x(t)]}{\sqrt{\Psi[\dot{x}(t)]}}. \tag{15}$$

However, Teager transform is an approximate estimation method. In order to improve the accuracy of Teager transform, there always follows a low-pass filter behind TEO. In this paper, the Teager transform is used to estimate instantaneous frequency and instantaneous amplitude of a signal.

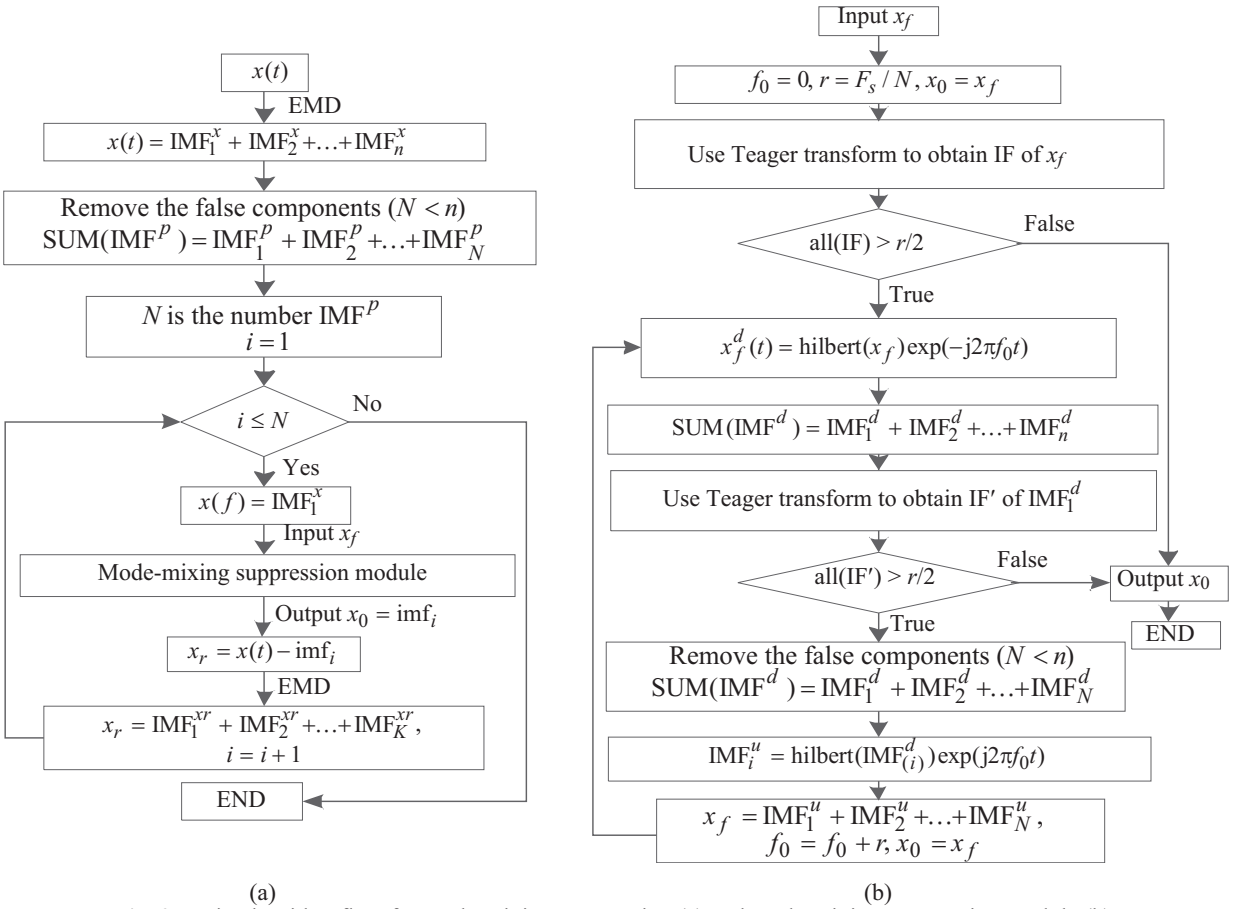

Fig. 2. Main algorithm flow for mode-mixing suppression (a) and mode-mixing suppression module (b).

3. SELF-FILTERING METHOD USING FREQUENCY CONVERSION TO SUPPRESS MODE MIXING

3.1. Reasons for Proposed Algorithm

According to the introduction above, mode mixing always occurs when the instantaneous frequencies of different signal components are closed. When the instantaneous frequencies are closed, $f_1 / f_2 \approx 1 < 2$. In order to increase the ratio, it is possible to subtract same frequency f_0 from f_1 and f_2 by down-converting the frequency of original signal, then the degree of mode mixing can be effectively suppressed.

Suppose that the frequency at crossing point E is f_I (Fig. 1), then the maximum down-converting frequency is close to f_I. After down-converting the frequency, use EMD method to obtain IMFs. Then use the same frequency to up-convert every IMF. In this way, a series of IMFs of original signal whose mode mixing is suppressed can be obtained. In most time signal composition is not known, so the frequency of the signal should be iteratively down-converted.

Although using the method of frequency conversion can effectively increase the ratio of the frequencies of different components around the intersection, there still exists some problem. When mode mixing seriously happens, the obtained IMFs always have lots of frequency errors. This is mainly due to the influence of IMFs whose frequencies are very low.

According to the introduction of EMD, the obtained IMFs are a series of data with high, sub-high, and low frequencies. By removing the IMFs containing low frequencies, it is possible to perform the adaptive filtering which is different from the commonly used filter. At the same time, the correlation coefficients between every IMF and the original signal have the same decreasing characteristic. The correlation coefficient between the first IMF and the original signal is largest. The correlation coefficient between the last IMF and the original signal is smallest. Hence this property can be used to improve the effect of modal mixing suppression. Every time after down-converting the frequency, IMFs with lower frequencies can be removed by removing the IMFs whose correlation coefficients are smaller with the down-converted signal.

3.2. Proposed Algorithm

In order to describe the process better, several variables are defined. The original signal is $x(t)$. The frequency resolution is r. The value of every time frequency change is f_0. The initial value of f_0 is 0. And the increment of f_0 is f_s. The main algorithm flow is as follows. Fig. 2(a) shows the main algorithm flow of the self-filtering method using frequency conversion. Fig. 2(b) shows the processing flow of the mode-mixing suppression module.

The algorithm starts from decomposing the $x(t)$ using EMD. The intrinsic mode functions of $x(t)$ are designated as IMF_i^x. Then $x(t)$ can be written as

$$x(t) = \sum_{i=1}^{n} \mathrm{IMF}_i^x. \tag{16}$$

Step 1. Calculate correlation coefficients between every x-th IMF and $x(t)$. Set a threshold "Thr1". In experiment Thr1 = 0.1. Define the components whose correlation coefficients are smaller than Thr1 as false components. Define the rest of IMF^x as primary components and designate it as IMF^p. The number of primary components is designated as N.

Step 2. Assign the first IMF_1^x, to x_f as the input data of mode-mixing suppression module. And the output data are designated as imf_1 whose mode mixing is suppressed. Then, imf_1 is the first intrinsic mode function of the original signal $x(t)$.

Step 3. Separate imf_1 from the rest of the signal by using

$$x(t) - \mathrm{imf}_1 = x_{r_1}. \tag{17}$$

Step 4. Decompose the x_{r_1} using EMD, and treat the first intrinsic mode function of x_{r_1} as x_f. Then repeat the process from step 3 to step 4 until imf_N is obtained. The result is

$$\begin{gathered} x_{r_1} - \mathrm{imf}_2 = x_{r_2} \\ \vdots \\ x_{r_{N-2}} - \mathrm{imf}_{N-1} = x_{r_{N-1}}. \end{gathered} \tag{18}$$

Then the primary components whose mode-mixing are suppressed of the original $x(t)$ are imf_1, imf_2, …, imf_N, and $x(t) = \sum_{i=1}^{N} \mathrm{imf}_N$, which is the designed EMD processing result with the proposed mode mixing suppression algorithm.

And the algorithm flow of mode-mixing suppression module is as follows. In the program, x_f is the original input data, and x_{out} is the final output data.

Step 1. Calculate the instantaneous frequency (IF) of x_f using Teager transform. Let x_{out} be equal to x_f. If there is any instantaneous frequency at specific time less than or equal to $r/2$, output x_{out} and end the program. Or else continue the program.

Step 2. Downshift the frequency of x_f, and the downshifted frequency is f_0. The obtained data $x_f^{d_1}$ is

$$x_f^{d_1} = \mathrm{hilbert}(x_f)\mathrm{e}^{-\mathrm{j}2\pi f_0 t}, \tag{19}$$

where "hilbert(…)" is the Hilbert transform.

Step 3. Decompose $x_f^{d_1}$ using EMD, and designate IMF^{d_1} as the obtained intrinsic mode function. Then calculate instantaneous frequency of $\mathrm{IMF}_1^{d_1}$.

Step 4. Check the instantaneous frequency (IF′) of $\mathrm{IMF}_1^{d_1}$. If there is any instantaneous frequency at specific time less than or equal to $r/2$, output x_{out} and end the program. Or else continue the program.

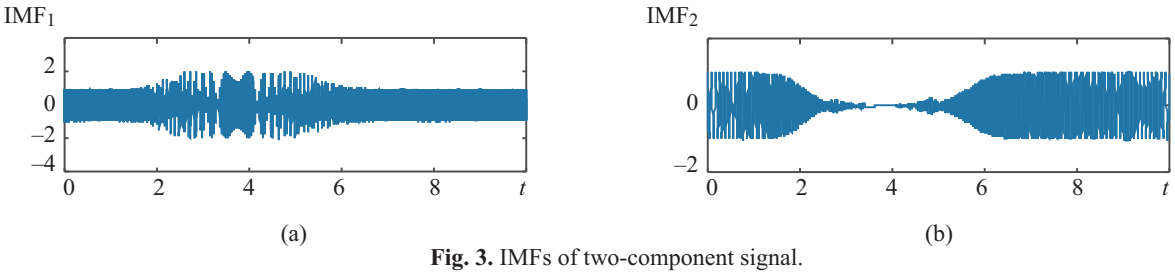

Fig. 3. IMFs of two-component signal.

Table 1. Improvement performance of two-component signal

Two-component signal	RMSE		Improvement, %
	before suppressing	after suppressing	
IMF_1	0.3875	0.1635	57.81
IMF_2	0.3865	0.1646	57.42

Table 2. Improvement performance of three-component signal

Three-component signal	RMSE		Improvement, %
	before suppressing	after suppressing	
IMF_1	0.4635	0.1465	68.40
IMF_2	0.6360	0.4048	36.36
IMF_3	0.5944	0.3777	36.47

Step 5. Remove the false components of IMF^{d_1}. Here set a threshold Thr2, and Thr2 can be smaller than Thr1. In experiment Thr2 = 0.07. Then up-convert the frequency of remaining intrinsic mode functions and obtain IMF^{u_1}. The up-converted frequency is same with the downshifted frequency in step 2

$$\mathrm{IMF}^{u_1} = \mathrm{hilbert}(\mathrm{IMF}^{d_1})\mathrm{e}^{\mathrm{j}2\pi f_0 t}. \tag{20}$$

Step 6. Treat the sum of IMF^{u_1} as new data x_f, and assign $f_0 + f_s$ to f_0. And let x_{out} be equal to new data x_f.

Step 7. Repeat the process from step 2 to step 6. And after K times of frequency downshift and frequency up conversion operation, the instantaneous frequencies of $\mathrm{IMF}_1^{d_K}$ can't satisfy the condition in step 4, that is, there are some instantaneous frequencies of $\mathrm{IMF}_1^{d_K}$ at specific time less than or equal to $r/2$, which shall happen. Then the result x_{out} is

$$x_{\mathrm{out}} = \sum_{i=1}^{K-1} \mathrm{IMF}^{u_i}, \tag{21}$$

where $\mathrm{IMF}^{u_i} = \mathrm{hilbert}(\mathrm{IMF}^{d_i})\mathrm{e}^{\mathrm{j}2\pi f_0 t}$.

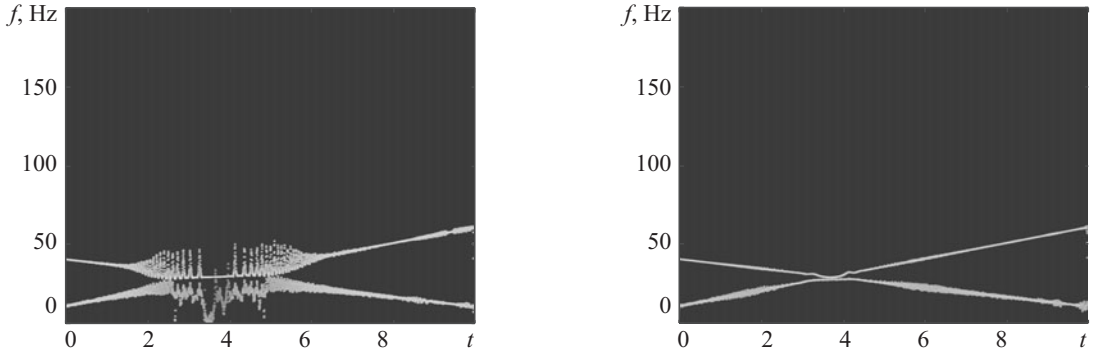

(a) (b)

Fig. 4. TFD spectrogram of two-component signal before (a) and after (b) mode-mixing suppression.

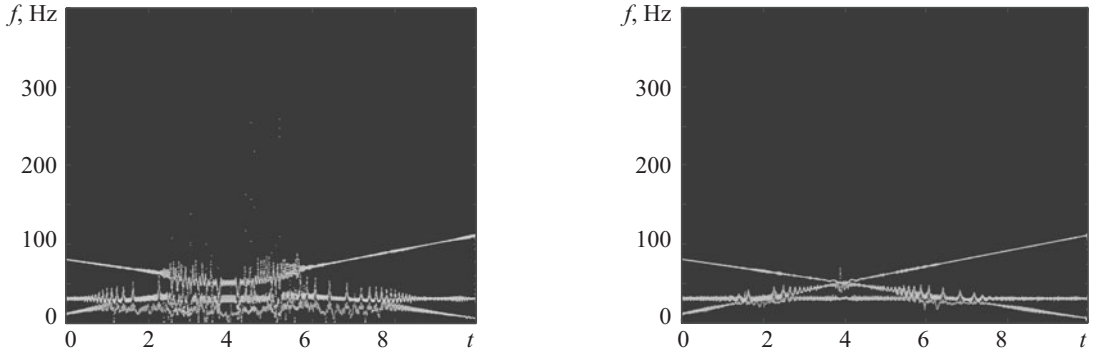

(a) (b)

Fig. 5. TFD spectrogram of three-component signal before (a) and after (b) mode-mixing suppression.

4. SIMULATION AND ANALYSIS

For a multi-component signal with two components we take the signal

$$x(t)=\cos(-3\pi t^2+80\pi t)+\cos(5\pi t^2+20\pi t) \tag{22}$$

as an example. The sampling frequency is 400 Hz.

The sample signal contains two signal components

$$x_1(t)=\cos(-3\pi t^2+80\pi t),$$

$$x_2(t)=\cos(5\pi t^2+20\pi t).$$

Decompose this signal using EMD. Fig. 3 shows the first two intrinsic mode functions. The figure shows severe mode mixing in IMF_1. The TFD spectrum of this two-component signal is shown in Fig. 4 from which an obvious mode mixing can be seen in the area where instantaneous frequencies intersect. Fig. 4(a) shows the time-frequency distribution spectrum obtained by self-filtering method using frequency conversion for empirical mode decomposition. It can be seen from Fig. 4(b) that the mode mixing region is significantly suppressed.

In order to illustrate the effect of suppression better, the root mean square error (RMSE) is used to evaluate the performance. According to the processing of EMD, the first IMF always contains the high-frequency components of a signal. Here, RMSE is defined between actual IMF and ideal IMF to illustrate the effect of inhibition. The smaller RMSE is, the closer the result of the decomposition is to the ideal result. The calculated results are shown in Tables 1, 2. Improvement percentage indicates the

Table 3. Comparison mode mixing suppression algorithms

Method	RMSE of IMF_1		RMSE of IMF_2	
	two-component signal	three-component signal	two-component signal	three-component signal
EEMD [31]	0.3872	0.4099	0.3863	0.6279
MS-EMD [29]	0.2543	0.1889	0.3334	0.6039
Proposed method	0.1658	0.1389	0.1646	0.3777

percentage reduction of RMSE after suppressing the mode mixing. The IMF obtained by the method proposed in this paper is much closer to the ideal IMF and, therefore, the performance is greatly improved.

For a multi-component signal with three components we take the signal

$$x(t) = \cos(-7.5\pi t^2 + 160\pi t) + \cos(10\pi t^2 + 20t\pi) + \cos(60\pi t) \tag{23}$$

as an example.

The signal $x(t)$ contains two frequency modulated signals and one mono-frequency signal. There are three intersections during the three frequencies of each signal component. The method proposed in this paper is used to suppress mode mixing. The results given in Fig. 5 show that the mode mixing is greatly suppressed.

Then the mask signal method [29] and EEMD method [31] are used to suppress mode mixing, and the RMSEs of first two IMFs are shown in Table 3. The table clearly shows that in the two-component and in the three-component signals, the RMSEs of IMF_1 and IMF_2 are both smaller for the proposed method as compared to the other methods. When comparing with mask method, the RMSE calculated using the proposed method is reduced by about 26%.

5. CONCLUSIONS

Empirical mode decomposition (EMD) is often accompanied by mode mixing during the processing of multi-component signals. Sometime mode mixing can greatly affect time-frequency distribution and further affect the detection of information. Based on the filter characteristics of EMD and combined with frequency conversion method, the mode mixing can be effectively suppressed that allows to get better time-frequency distribution spectrogram, which is conducive to improving the accuracy of frequency information detection. Comparing with EEMD and mask method, the mode mixing suppression using the proposed method can be improved by about 26%.

CONFLICT OF INTEREST

The authors declare that they have no conflict of interest.

ADDITIONAL INFORMATION

The initial version of this paper in Russian is published in the journal “Izvestiya Vysshikh Uchebnykh Zavedenii. Radioelektronika,” ISSN 2307-6011 (Online), ISSN 0021-3470 (Print) on the link http://radio.kpi.ua/article/view/S0021347019090036 with DOI: 10.20535/S0021347019090036.

REFERENCES

1. L. Stankovic, S. Stankovic, M. Dakovic, "From the STFT to the Wigner distribution [Lecture Notes]," *IEEE Signal Proces. Mag.* **31**, No. 3, 163 (2014). DOI: 10.1109/MSP.2014.2301791.
2. M. A. Awal, S. Ouelha, S. Y. Dong, B. Boashash, "A robust high-resolution time-frequency representation based on the local optimization of the short-time fractional Fourier transform," *Digital Signal Processing* **70**, 125 (Nov. 2017). DOI: 10.1016/j.dsp.2017.07.022.
3. I. Daubechies, "The wavelet transform, time-frequency localization and signal analysis," *IEEE Trans. Inf. Theory* **36**, No. 5, 961 (1990). DOI: 10.1109/18.57199.
4. B. Boashash, "Note on the use of the Wigner distribution for time-frequency signal analysis," *IEEE Trans. Acoustics, Speech, Signal Processing* **36**, No. 9, 1518 (1988). DOI: 10.1109/29.90380.
5. T. Claasen, W. Mecklenbrauker, "Time-frequency signal analysis by means of the Wigner distribution," *Proc. of ICASSP'81. IEEE Int. Conf. on Acoustics, Speech, and Signal Processing*, 30 Mar.-1 Apr. 1981, Atlanta, USA (IEEE, 1981), pp. 69-72. DOI: 10.1109/ICASSP.1981.1171331.
6. D. Chan, "A non-aliased discrete-time Wigner distribution for time-frequency signal analysis," *Proc. of ICASSP'82. IEEE Int. Conf. on Acoustics, Speech, and Signal Processing*, 3-5 May 1982, Paris, France (IEEE, 1982), pp. 1333-1336. DOI: 10.1109/ICASSP.1982.1171451.
7. H. Hu, "Time-frequency DOA estimate algorithm based on SPWVD," *Proc. of 2005 IEEE Int. Symp. on Microwave, Antenna, Propagation and EMC Technologies for Wireless Communications*, 8-12 Aug. 2005, Beijing, China (IEEE, 2005), Vol. 2, pp. 1253-1256. DOI: 10.1109/mape.2005.1618151.
8. O. Y. Sorokin, "Increase of efficiency of spread spectrum radio signals application in communication systems," *Radioelectron. Commun. Syst.* **55**, No. 1, 38 (2012). DOI: 10.3103/S0735272712010062.
9. B. Barkat, B. Boashash, "A high-resolution quadratic time-frequency distribution for multicomponent signals analysis," *IEEE Trans. Signal Processing* **49**, No. 10, 2232 (2001). DOI: 10.1109/78.950779.
10. A. P. Gvozdak, "Detection of nonstationary components of signals with the use of distributions based on kernels with affine transforms," *Radioelectron. Commun. Syst.* **48**, No. 8, 31 (2005). URI: http://radioelektronika.org/article/view/S0735272705080066.
11. W. Martin, P. Flandrin, "Wigner-Ville spectral analysis of nonstationary processes," *IEEE Trans. Acoustics, Speech, and Signal Processing* **33**, No. 6, 1461 (1985). DOI: 10.1109/TASSP.1985.1164760.
12. H.-L. Chan, H.-H. Huang, J.-L. Lin, "Time-frequency analysis of heart rate variability during transient segments," *Annals Biomedical Engineering* **29**, No. 11, 983 (Nov. 2001). DOI: 10.1114/1.1415525.
13. H. Hang, "Time-frequency DOA estimation based on Radon-Wigner transform," *Proc. of 2006 8th Int. Conf. on Signal Processing*, 16-20 Nov. 2006, Beijing, China (IEEE, 2006), p. 1. DOI: 10.1109/ICOSP.2006.344553.
14. M. Amirmazlaghani, H. Amindavar, "Modeling and denoising Wigner-Ville distribution," *Proc. of 2009 IEEE 13th Digital Signal Processing Workshop and 5th IEEE Signal Processing Education Workshop*, 4-7 Jan. 2009, Marco Island, USA (IEEE, 2009), pp. 530-534. DOI: 10.1109/DSP.2009.4785980.
15. N. E. Huang, Z. Shen, S. R. Long, M. C. Wu, H. H. Shih, Q. Zheng, N.-C. Yen, C. C. Tung, H. H. Liu, "The empirical mode decomposition and the Hilbert spectrum for nonlinear and non-stationary time series analysis," *Proc. Royal Soc. A - Math. Phys. Engineering Sci.* **454**, No. 1971, 903 (Mar. 1998). DOI: 10.1098/rspa.1998.0193.
16. B. L. Cheng, A. N. Kubrak, "Modernized method of estimating the parameters of LFM signals based on the time-frequency distribution correction and the use of the Hough transformation," *Radioelectron. Commun. Syst.* **52**, No. 6, 295 (2009). DOI: 10.3103/S0735272709060028.
17. J. D. Zheng, J. S. Cheng, Y. Yang, "Partly ensemble empirical mode decomposition: An improved noise-assisted method for eliminating mode mixing," *Signal Processing* **96**, Part B, 362 (Mar. 2014). DOI: 10.1016/j.sigpro.2013.09.013.
18. H. Quan, Z. Liu, X. Shi, "A new processing method for the end effect problem of empirical mode decomposition," *Proc. of 2010 3rd Int. Congress on Image and Signal Processing*, 16-18 Oct. 2010, Yantai, China (IEEE, 2010), pp. 3391-3394. DOI: 10.1109/CISP.2010.5647347.
19. P. Y. Kovalenko, D. I. Bliznyuk, A. S. Berdin, "Improved extrema detection algorithm for the generalized empirical mode decomposition," *Proc. of 2nd Int. Conf. on Industrial Engineering, Applications and Manufacturing*, ICIEAM, 19-20 May 2016, Chelyabinsk, Russia (IEEE, 2016), pp. 1-5. DOI: 10.1109/ICIEAM.2016.7911546.
20. Peng Wang, Guo-chu Chen, Yu-fa Xu, Jin-shou Yu, "Improved empirical mode decomposition and its application to wind power forecasting," *Control Engineering China* **18**, No. 4, 588 (2011). URI: https://caod.oriprobe.com/articles/28044593/Improved_Empirical_Mode_Decomposition_and_its_Appl.htm.
21. Zhi-meng Zhang, Chen-chen Liu, Bo-sheng Liu, Bao-jing Tian, "Simulation analysis of envelops fitting algorithms in EMD," *J. System Simulation* **21**, No. 23, 7690 (2009). URI: http://caod.oriprobe.com/articles/38656675/jing_yan_mo_tai_fen_jie_zhong_de_bao_luo_xian_ni_he_suan_fa_fang_zhen_.htm.
22. O. V. Lazorenko, L. F. Chernogor, "System spectral analysis of infrasonic signal generated by Chelyabinsk meteoroid," *Radioelectron. Commun. Syst.* **60**, No. 8, 331 (2017). DOI: 10.3103/S0735272717080015.
23. M. Svoboda, L. Matiu-Iovan, F. M. Frigura-Iliasa, P. Andea, "B-spline interpolation technique for digital signal processing," *Proc. of 2015 Int. Conf. on Information and Digital Technologies*, 7-9 Jul. 2015, Zilina, Slovakia (IEEE, 2015), pp. 366-371. DOI: 10.1109/DT.2015.7222998.

24. Q. Chen, N. Huang, S. Riemenschneider, Y. Xu, "A B-spline approach for empirical mode decompositions," *Adv. Comput. Math.* **24**, No. 1-4, 171 (2006). DOI: 10.1007/s10444-004-7614-3.
25. J. H. Shixi Yang, Zhaotong Wu, et al. "Study of empirical mode decomposition based on high-order spline interpolation," *J. Zhejiang University: Engineering Sci.* **38**, No. 3, 267 (2004).
26. H. Ding, J. Lv, "Comparison study of two commonly used methods for envelope fitting of empirical mode decomposition," *Proc. of 2012 5th Int. Congress on Image and Signal Processing*, 16-18 Oct. 2012, Chongqing, China (IEEE, 2012), pp. 1875-1878. DOI: 10.1109/CISP.2012.6469862.
27. D. J. Huang, J. P. Zhao, J. L. Su, "Practical implementation of Hilbert-Huang Transform algorithm," *Acta Oceanologica Sinica* **22**, No. 1, 1 (2003). URI: http://www.hyxb.org.cn/aoscn/ch/reader/view_abstract.aspx?file_no=20030101&flag=1.
28. N. E. Huang, Z. Shen, S. R. Long, "A new view of nonlinear water waves: The Hilbert spectrum," *Annual Review Fluid Mech.* **31**, 417 (1999). DOI: 10.1146/annurev.fluid.31.1.417.
29. R. Deering, J. F. Kaiser, "The use of a masking signal to improve empirical mode decomposition," *Proc. of IEEE Int. Conf. on Acoustics, Speech, and Signal Processing*, 23 Mar. 2005, Philadelphia, USA (IEEE, 2005), Vol. 4, pp. iv/485-iv/488. DOI: 10.1109/ICASSP.2005.1416051.
30. Y. Gao, G. Ge, Z. Sheng, E. Sang, "Analysis and solution to the mode mixing phenomenon in EMD," *Proc. of 2008 Congress on Image and Signal Processing*, 27-30 May 2008, Sanya, Hainan, China (IEEE, 2008), pp. 223-227. DOI: 10.1109/CISP.2008.193.
31. Z. Wu, N. E. Huang, "Ensemble empirical mode decomposition: A noise-assisted data analysis method," *Advances in Adaptive Data Analysis* **01**, No. 01, 1 (2009). DOI: 10.1142/s1793536909000047.
32. N. Senroy, S. Suryanarayanan, P. F. Ribeiro, "An improved Hilbert-Huang method for analysis of time-varying waveforms in power quality," *IEEE Trans. Power Systems* **22**, No. 4, 1843 (Nov. 2007). DOI: 10.1109/tpwrs.2007.907542.
33. N. E. Huang, M.-L. C. Wu, S. R. Long, S. S. P. Shen, W. Qu, P. Gloersen, K. L. Fan, "A confidence limit for the empirical mode decomposition and Hilbert spectral analysis," *Proc. of Royal Soc. A - Math. Phys. Eng. Sci.* **459**, No. 2037, 2317 (Sep. 8 2003). DOI: 10.1098/rspa.2003.1123.
34. N. Stevenson, M. Mesbah, B. Boashash, "A sampling limit for the empirical mode decomposition," *Proc. of Eighth Int. Symp. on Signal Processing and Its Applications*, 28-31 Aug. 2005, Sydney, Australia (IEEE, 2005), pp. 647-650. DOI: 10.1109/ISSPA.2005.1581021.
35. G. Rilling, P. Flandrin, "One or two frequencies? The empirical mode decomposition answers," *IEEE Trans. Signal Processing* **56**, No. 1, 85 (Jan. 2008). DOI: 10.1109/Tsp.2007.906771.
36. B. Boashash, "Estimating and interpreting the instantaneous frequency of a signal. II. Algorithms and applications," *Proc. IEEE* **80**, No. 4, 540 (1992). DOI: 10.1109/5.135378.
37. J.-C. Cexus, A.-O. Boudraa, "Nonstationary signals analysis by Teager-Huang Transform (THT)," *Proc. of 14th European Signal Processing Conf.*, 4-8 Sept. 2006, Florence, Italy (IEEE, 2006), pp. 1-5. URI: https://ieeexplore.ieee.org/document/7071680.
38. S. Benramdane, J. C. Cexus, A. O. Boudraa, J.-A. Astolfi, "Time-frequency analysis of pressure fluctuations on a hydrofoil undergoing a transient pitching motion using Hilbert-Huang and Teager-Huang transforms," *Proc. of Asme Pressure Vessels and Piping Conf.*, 22-26 Jul. 2007, San Antonio, USA (IEEE, 2008), Vol. 4: Fluid-Structure Interaction, pp. 199-207. DOI: 10.1115/PVP2007-26632.
39. M. F. Kaleem, L. Sugavaneswaran, A. Guergachi, S. Krishnan, "Application of empirical mode decomposition and Teager energy operator to EEG signals for mental task classification," *Proc. of 2010 Annual Int. Conf. of IEEE Engineering in Medicine and Biology*, 31 Aug.-4 Sept. 2010, Buenos Aires, Argentina (IEEE, 2010), pp. 4590-4593. DOI: 10.1109/IEMBS.2010.5626501.
40. J. Guo, S. Qin, C. Zhu, "The application of energy operator demodulation approach based on EMD in mechanical system identification," *Proc. of 19th Int. Conf. on Mechatronics and Machine Vision in Practice*, M2VIP, 28-30 Nov. 2012, Auckland, New Zealand (IEEE, 2012), pp. 80-85. URI: https://ieeexplore.ieee.org/document/6484571.
41. H. Li, H. Zheng, L. Tang, "Gear fault diagnosis based on order tracking and Hilbert-Huang transform," *Proc. of 2009 Sixth Int. Conf. on Fuzzy Systems and Knowledge Discovery*, 14-16 Aug. 2009, Tianjin, China (IEEE, 2009), pp. 468-472. DOI: 10.1109/FSKD.2009.220.